Plant Physiology and Biochemistry 206 (2024) 108270

Contents lists available at ScienceDirect

Plant Physiology and Biochemistry

journal homepage: www.elsevier.com/locate/plaphy

Are tomato plants co-exposed to heat and salinity able to ensure a proper carbon metabolism? – An insight into the photosynthetic hub

Francisca Rodrigues [a,b,#,1], Bruno Sousa [a,*,1], Cristiano Soares [a], Diana Moreira [c], Cláudia Pereira [a], José Moutinho-Pereira [d], Ana Cunha [b], Fernanda Fidalgo [a]

[a] GreenUPorto – Sustainable Agrifood Production Research Centre and INOV4AGRO, Department of Biology, Faculty of Sciences of University of Porto, Rua do Campo Alegre s/n, 4169-007 Porto, Portugal
[b] Biology Department and CBMA – Centre of Molecular and Environmental Biology, School of Sciences of University of Minho, Campus de Gualtar, 4710-057 Braga, Portugal
[c] LAQV/REQUIMTE, Department of Biology, Faculty of Sciences of University of Porto, Rua do Campo Alegre s/n, 4169-007 Porto, Portugal
[d] CITAB - Centre for the Research and Technology of Agro-Environmental and Biological Sciences, Universidade de Trás-os-Montes e Alto Douro, 5000-801 Vila Real, Portugal

ARTICLE INFO

Keywords:
Solanum lycopersicum
Abiotic stress
Photochemistry
Chlorophyll fluorescence
Photosystem II
Gas exchange
Heat shock response

ABSTRACT

Abiotic stress combinations, such as high temperatures and soil/water salinization, severely threaten crop productivity worldwide. In this work, an integrative insight into the photosynthetic metabolism of tomato plants subjected to salt (100 mM NaCl) and/or heat (42 °C; 4 h/day) was performed. After three weeks, the stress combination led to more severe consequences on growth and photosynthetic pigments than the individual stresses. Regarding the photochemical efficiency, transcript accumulation and protein content of major actors (CP47 and D1) were depleted in all stressed plants, although the overall photochemical yield was not negatively affected under the co-exposure. Gas-exchange studies revealed to be mostly affected by salt (single or combined), which harshly compromised carbon assimilation. Additionally, transcript levels of stress-responsive genes (*e.g.*, *HsfA1* and *NHX2*) were differentially modulated by the single and combined treatments, suggesting the activation of stress-signature responses. Overall, by gathering an insightful overview of the main regulatory hub of photosynthesis, we show that the impacts on the carbon metabolism coming from the combination of heat and salinity, two major conditioners of crop yields, were not harsher than those of single stresses, indicating that the growth impairment might be attributed to a proficient distribution of resources towards defense mechanisms.

1. Introduction

Sessile organisms, such as plants, highly rely on their incredible plasticity to develop under adverse conditions (Zhang et al., 2021). However, the current climatic instability, coupled with anthropic-related environmental degradation, has been gradually – yet now at an unsettlingly accelerated pace – propelling agriculture past its limitations, since plants are not able to adapt in due time to these drastic abiotic fluctuations.

Tomato (*Solanum lycopersicum* L.) fruit is one of the most produced and consumed goods within the Iberian Peninsula. Indeed, both Spain and Portugal regularly secure positions within the five biggest annual producers in Europe. However, recent years have witnessed a decline in tomato cultivation in these regions (Eurostat, 2021), this being most likely correlated with the impacts of an ever-shifting climate, a concern further amplified by the projections of the latest report of the Intergovernmental Panel on Climate Change (IPCC, 2021). According to it, before the year 2100, a rise in average temperature up to 5 °C in the Mediterranean area can be expected, with ~30 days each year reaching a maximum temperature over 40 °C, largely surpassing the 25–35 °C threshold for heat stress in most crops (Wahid et al., 2007). As a consequence of global warming, agricultural practises increasingly demand higher irrigation requirements, thus pushing the utilization of suboptimal water resources. All of this can result in long-term soil

* Corresponding author. Sustainable Agrifood Production Research Centre and INOV4AGRO, Department of Biology, Faculty of Sciences of University of Porto, Rua do Campo Alegre s/n, 4169-007 Porto, Portugal.
E-mail address: bruno.filipe@fc.up.pt (B. Sousa).
Present address: InnovPlantProtect, Estrada de Gil Vaz, Apartado 72 7351-901 Elvas, Portugal.
[1] These authors contributed equally for this research and should both be considered as first authors.

https://doi.org/10.1016/j.plaphy.2023.108270
Received 28 August 2023; Received in revised form 7 November 2023; Accepted 6 December 2023
Available online 10 December 2023

salinization, compromising agricultural yield and further escalating the concerning scenario of desertification in the Mediterranean basin (Haddeland et al., 2014; Koutroulis et al., 2013; Daliakopoulos et al., 2016). To face these issues, plant stress research must shift towards understanding the crosstalk between heat and salinity effects on crop performance, as well as focusing on identifying putative tolerance mechanisms in order to promote a sustainable, yet profitable, agricultural chain. Being considered as the "power factory" of photoautotrophic organisms, the importance of the photosynthetic machinery should not be understated. Thus, upon disruption of this metabolic process, which is highly sensitive to environmental shifts, including changes in temperature and soil salt levels (Singh et al., 2018; Parihar et al., 2015; Mathur et al., 2014; Hassan et al., 2021), plant survival can be threatened and crop productivity put at risk. A common consequence of both salt and heat stress is the disruption of the chloroplast organization, as well as the increased degradation or inhibited production of chlorophylls and carotenoids, while also leading to defects in water relations, photochemical reactions, carbon metabolism and net photosynthetic rate, stomatal conductance, and protein biosynthesis, including Ribulose-1,5-bisphosphate carboxylase-oxygenase (RuBisCO; EC 4.1.1.39), the main enzyme responsible for carbon assimilation (Singh et al., 2018; Parihar et al., 2015; Mathur et al., 2014; Hassan et al., 2021; Zahra et al., 2022; Zahra et al., 2023).

In an attempt to survive under these unfavorable conditions, plants must quickly respond and adapt, activating a series of coordinated molecular, biochemical, morphophysiological responses. Under abiotic stress exposure, heat shock proteins (HSPs) are important molecular chaperones responsible for protein stabilization and refolding after stress events (Al-Whaibi, 2011; Park and Seo, 2015). Moreover, specifically in the case of salinity, plants need also to employ strategies to avoid ionic toxicity, either by inhibiting salt uptake and translocation, or by favouring its compartmentalization, regulated by ion transporters, such as the NHX (Na^+/H^+ antiporters) class (Parihar et al., 2015). These transporters are major regulators of active potassium (K) uptake and turgor potential, thus preventing the accumulation of toxic ions in plant cells, and maintaining K^+/Na^+ homeostasis (Parihar et al., 2015). Nonetheless, and although the overall defense network can be enough to at least partially deal with slight to moderate stress episodes, strong and/or chronic exposures can be more harmful and still affect plant development. This is especially worrying because, in the context of climate change, the severity, frequency and combination of stressors are increasing, leading to consequences that can differ, and be harsher, than the effects of the sum of each one (Suzuki et al., 2014). Recently, the studies conducted by Rivero et al. (2014) and Lopez-Delacalle et al. (2021) observed that the behaviour of tomato plants treated with salt (hydroponics, 120 mM for 72 h or 75 mM NaCl for 14 days, respectively) and heat (35 °C) was similar to those exposed only to high temperatures and showed to be less affected than by the salt treatment, at least regarding growth and photosynthesis. Contrastingly, using a different experimental design (based on the current projections for the Mediterranean), results published by our research team (Sousa et al., 2022), indicate that the performance of potted tomato plants exposed to the combined stress (irrigated with 100 mM NaCl, and exposed daily to 42 °C for 4 h during 3 weeks) is more severely affected than what could be expected from the individual effects. In light of this information, it is clear that there is still much more to learn concerning this subject, especially the intracellular and biochemical pathways involved in the crosstalk between salinity and heat.

Thus, considering our previous studies, we hypothesize that the high growth inhibition found in tomato plants co-exposed to heat and salinity can result from an impaired photosynthetic performance and a down-regulation of defensive pathways related to nutrient homeostasis, rather than oxidative damage, as recently shown (Sousa et al., 2022).

To test these hypotheses, this work mainly aims to assess the consequences of the co-exposure to heat and salt on the photosynthetic apparatus of *S. lycopersicum* plants, by analysing several endpoints such as a) the evaluation of photosynthetic pigments and RuBisCO and D1 – both at the protein and gene level; b) chlorophyll fluorescence analysis; and c) gas-exchange measurements. To complement this approach, the histochemical detection of cell death and the expression of genes related to the heat shock response, as well as ion transporters (NHX), were also conducted to better understand the response of *S. lycopersicum* to this stress combination, which is set to become increasingly common in the Mediterranean region.

2. Material and methods

2.1. Plant growth and experimental design

Seeds of cherry tomato (*Solanum lycopersicum* L. var *cerasiforme*) underwent a surface disinfection process with 70% (v/v) ethanol (7 min) and 20% (v/v) commercial bleach [5% active chloride and 0.02% (w/v) tween-20] (5 min). Then, seeds were washed several times with deionized water (dH_2O) to remove the excess of disinfectants. Subsequently, seeds were evenly spread in Petri dishes filled with solid (0.675% w/v agar) half-strength MS (Murashige and Skoog, 1962) growth medium with Gamborg B5 (Gamborg et al., 1968) vitamins (Sigma-Aldrich®, Steinheim, Germany). Seeds were then germinated, for 7 days, in a growth chamber [16 h light/8 h dark photoperiod, photosynthetic photon flux density (PPFD) of 150 μmol m^{-2} s^{-1}, 25 °C]. Afterwards, seedlings were planted and grown under the controlled conditions above-mentioned, on pots containing Siro Royal universal substrate (SIRO©, Portugal; characterized in Table S1 of Sousa et al. (2022)). For the first 7 days, seedlings were irrigated only with dH_2O to allow them to acclimate to pot conditions. For each condition, four pots (defined as the biological replicate), each one with three plants, were considered.

After the acclimation week, pots were randomly divided into different trays (4 pots per tray) and plants were grown for the next 3 weeks with these experimental groups:

- **CTL –** control plants, only irrigated with dH_2O (60 mL for each pot every two days) and grown under 25 °C;
- **SALT –** salt-treated plants, irrigated, every two days, with a 100 mM NaCl solution (60 mL for each pot) and grown under 25 °C;
- **HEAT –** heat-exposed plants, only irrigated with dH_2O (60 mL for each pot every two days) and daily exposed, for 4 h, to 42 °C in a twin growth chamber;
- **COMBINED –** co-exposed plants, irrigated, every two days, with a 100 mM NaCl solution (60 mL for each pot) and daily exposed, for 4 h, to 42 °C in a twin growth chamber.

This experimental design was selected based on our previously published work (Sousa et al., 2022), being also aligned with former literature (Ayers and Westcot, 1985) and with the predicted future climatic trends for the Mediterranean basin (Carvalho et al., 2021). Heat stress was applied between the 5th and 9th hours of light, mimicking similar conditions to those observed under a real scenario.

After 3 weeks of exposure, gas exchange determinations, chlorophyll fluorometry, and cell death analysis were carried out *in vivo* in the 2nd and 3rd fully expanded leaves of every plant. Afterwards, plants were collected, thoroughly washed, and the aerial portion of some plants was frozen and macerated in liquid nitrogen and stored at −80 °C for molecular and biochemical determinations.

2.2. Cell viability - histochemical determination

Fully expanded leaves (2nd and 3rd) from plants of each condition were processed as detailed in Soares et al. (2016). In summary, leaves were incubated for 4 h in 0.25% (w/v) Evans Blue, in the dark, and then decolorized with 96% (v/v) boiling ethanol. Lastly, after being carefully washed, leaves were photographed. Since Evans Blue cannot enter viable cells, the occurrence of blueish areas indicates loss of cell

viability.

2.3. Determination of chlorophylls and carotenoids levels

The determination of the levels of photosynthetic pigments was carried out in accordance with the method of Lichtenthaler (1987). Here, frozen samples were macerated in 80% (v/v) acetone and absorbances were read at 664, 647, and 470 nm, after a 10 min-centrifugation. Chlorophyll (*a* and *b*) and carotenoids were calculated trough the formulas of Lichtenthaler (1987). Results were expressed in mg g^{-1} dry weight (dw), estimated from the calculated water content (Sousa et al., 2022).

2.4. Chlorophyll fluorometry

2.4.1. Photochemical efficiency of photosystem II (PSII) - maximum quantum yield (F_v/F_m), relative electron transport rate (rETR), PSII efficiency (ΦPSII), and non-photochemical quenching (NPQ)

Chlorophyll fluorescence parameters were analysed [as described in Soares et al. (2020)], through pulse-amplitude modulated (PAM) fluorometry, in the 2nd and 3rd expanded leaves, with a PAM-210 fluorometer (Heinz Walz GmbH, 1997), controlled with the PAMWin software. This equipment possessed a far red LED [long-pass filter (>710 nm ad with a peak at ~730 nm)], an actinic red LED (unfiltered, with a peak at ~665 nm), a red measuring LED [short-pass filter (<690 nm)] and a PIN photodiode and dichroic filter, which reflect fluorescence to the detector at a 90° angle.

Plants were kept in obscurity for over half an hour so that all the PSII reaction centres were open. Afterwards, minimal fluorescence (F_0) was recorded before applying a saturating light pulse (PPFD: 3500 μmol m^{-2} s^{-1}, 800 ms), which allowed the detection of maximum fluorescence (F_m) and the calculation of the maximum PSII quantum yield (F_v/F_m=(F_m–F_0)/F_m (Kitajima and Butler, 1975). Then, after a 10 min adaptation to an actinic light with similar light intensity to that of the growth chamber (128 μmol m^{-2} s^{-1}), a saturating light pulse was applied, allowing the determination of the steady-state fluorescence (F_t) and maximum fluorescence yield (F'_m). Here, relative electron transport rate (rETR = Φ_{PSII} x PPFD) and effective PSII quantum yield [Φ_{PSII} = (F'_m-F_t)/F'_m] (Genty et al., 1989) were calculated. Non-photochemical quenching (NPQ) was determined as (F_m–F'_m)/F'_m (Muller et al., 2001).

2.4.2. Rapid light curves (RLC)

Immediately after the above-mentioned quantifications (2.4.1), the same leaves were subjected to eleven increasing actinic light levels for 20 s (PPFD: 18, 68, 98, 128, 158, 218, 318, 448, 608, 858 and 1258 μmol m^{-2} s^{-1}). After each step, leaves were exposed to a saturating pulse to calculate the respective Φ_{PSII}, rETR and NPQ.

2.5. Gas-exchange measurements

An infrared gas analysed (IRGA; LCpro$^+$, ADC, Hodderson, UK), coupled to a broad light source was used to evaluate gas-exchange parameters, simulating greenhouse conditions (atmospheric CO_2 concentration, PPFD of 128 μmol m^{-2} s^{-1}). Measurements were carried out in fully expanded leaves of plants from every biological replicate. Net CO_2 assimilation rate (P_N, μmol m^{-2} s^{-1}), stomatal conductance (g_s, mmol m^{-2} s^{-1}), transpiration rate (*E*, mmol m^{-2} s^{-1}), and intracellular/atmospheric CO_2 (C_i/C_a) were calculated through the equations of von Caemmerer and Farquhar (von Caemmerer and Farquhar, 1981). Moreover, specific leaf area [*SLA* = leaf area (cm^2)/dw (g)] and intrinsic water use efficiency ($WUE_i = P_N/g_s$.) were also evaluated. Since SLA was altered by the different treatments, all gas exchange parameters were expressed based on mass (mol g^{-1} s^{-1}) instead of area (mol m^{-2} s^{-1}).

2.6. RT-qPCR gene expression analysis

2.6.1. RNA extraction and purification and cDNA synthesis

Total RNA was extracted from frozen shoot samples with the NZYol (NZytech®, Portugal) reagent, according to the suppliers's instructions. Then, the GRS Total RNA kit – Plant from GRiSP® (GRiSP Research Solutions, Portugal), which includes a DNAse I step, was utilized to purify the extracted RNA. Upon these steps, RNA levels (1.0 $Abs_{260\ nm}$ = 40 ng μL^{-1}) and purity ($Abs_{260/280\ nm}$ and $Abs_{260/230\ nm}$) were determined with a DS-11 Microvolume Abs Spectrophotometer (DeNovix Inc., USA). RNA integrity was analysed by agarose gel electrophoresis. Afterwards, cDNA synthesis was achieved through the Xpert cDNA Synthesis Kit (GRiSP®), with 1 μg of RNA (20 μL total volume). Samples were stored at −20 °C before being used for real-time PCR (qPCR).

2.6.2. qPCR analysis of gene expression

Through a qPCR analysis, the transcript accumulation for a range of genes associated with photosynthesis (Table 1) or responsive to salt or heat stress conditions (Table 2) was determined. *D1* and *CP47* are responsible for encoding proteins linked to the reaction centre of PSII, whereas *RbcL* and *RbcS* code for the large and small subunits of RuBisCO, respectively. The reactions were carried out, in triplicate, on a CFX96 Real-Time Detection System (Bio-Rad®, Portugal). In every reaction (20 μL), the following components were added: 1x PowerUp™ SYBR® Green Master Mix, 0.4 μM primers (Tables 1 and 2) and 1 μL of diluted (1:10) cDNA. The qPCR cycle was: 50 °C for 2 min, 95 °C for 2 min, 35 cycles of 95 °C for 3, 60 °C (Table 1) or 57 °C (Table 2) for 30 s. Melting curve analysis was done with a 60–95 °C range, at 0.5 °C increments, to assess primer specificity, showing an individual peak for each gene. The obtained data was normalized through the $2^{(-\Delta\Delta Ct)}$ formula (Livak and Schmittgen, 2001), using *UBIQUITIN* and *ACTIN* as reference genes (Løvdal and Lillo, 2009).

2.7. Western blotting analysis of RbcL and D1

Soluble proteins from frozen shoot samples were extracted, under ice-cold conditions, as described in Sousa et al. (2022). Total soluble protein content was then determined spectrophotometrically (at 595 nm) according to the Bradford method (Bradford, 1976), using different concentrations of bovine serum albumin for the calibration curve. Four parts of the protein sample were then mixed with one part of 5x SDS-PAGE Sample Loading Buffer (NZytech®, Portugal) and incubated at 100 °C for 5 min. After a quick centrifugation, samples were allowed to cool down to room temperature before being used for western blotting.

SDS-PAGE was performed using a 12.5% polyacrylamide gel (Laemmli, 1970), loading the volume containing 15 μg of each protein extract. BLUE Wide Range CSL-BBL Prestained Protein Ladder (Cleaver Scientific Ltd) was used as a protein molecular weight marker. Following electrophoresis, proteins were transferred to a nitrocellulose membrane through the Trans-Blot Turbo Transfer System (Biorad®), with a buffer containing 25 mM Tris, 192 mM glycine, and 20% (v/v) methanol. Then, the membrane was blocked for 30 min, under constant agitation, in TBS-T buffer [20 mM Tris, 150 mM NaCl, 0.1% (w/v) Tween®20] supplemented with 5% (w/v) skim milk and subsequently incubated overnight at 4 °C, under constant rotation, with antibodies raised against PsbA/D1 (AS05 084, Agrisera, Sweden) or RbcL (AS03 037, Agrisera, Sweden), diluted to 1:10 000 and 1:7 500, respectively. The housekeeping protein tubulin (AS10 680, Agrisera, Sweden), diluted 1:1 000, was used as an internal loading control. Membranes were then washed three times with TBS-T buffer before incubating for 1 h, under constant rotation, with anti-Rabbit IgG (H&L), HRP conjugated (AS09 602, Agrisera, Sweden), diluted to 1:10 000. Then, membranes were washed three times with TBS-T and one time with dH_2O. The reaction was then revealed using Clarity Western ECL Blotting Substrate and imaged through a Chemidoc™ XRS + System (Biorad®), with the

Table 1
Forward (Fwd) and reverse (Rev) qPCR primers for genes related to photosynthesis, along with the respective amplicon size and melting temperature.

Name	Sequence	Amplicon Size (bp)	Melting Temperature (° C)	Reference
D1	**Fwd:** TGGATGGTTTGGTGTTTTGATG	191	54.03	Mariz-Ponte et al. (2021)
	Rev: CCG TAAAGTAGAGACCCTGAAAC		54.83	
CP47	**Fwd:** CCTATTCCATCTTAGCGTCCG	142	54.90	
	Rev: TTGCCGAACCATACCACATAG		54.87	
RbcS	**Fwd:** TGAGACTGAGCACGGATTTG	148	54.90	
	Rev: TTTAGCCTCTTGAACCTCAGC		54.79	
RbcL	**Fwd:** ATCTTGCTCGGGAAGGTAATG	81	54.68	
	Rev: TCTTTCCATACCTCACAAGCAG		54.64	

Table 2
Forward (Fwd) and reverse (Rev) qPCR primers for stress-related genes, along with the respective amplicon size and melting temperature.

Name	Sequence	Amplicon Size (bp)	Melting Temperature (° C)
HsfA1	**Fwd:** GCAGTTGAGGGAAAAGTGGG	159	59.04
	Rev: ATCAGGGGAACAAGGGCTTT		59.21
HsfA2	**Fwd:** CAATGTCAGGCCGGATTCTG	125	58.98
	Rev: CTACTTCCTCTGCTGCTCGA		58.9
Hsp70	**Fwd:** TAAGGTGCCTGCTGACGTAA	193	59.03
	Rev: TGTACCAGCACCAGGAGAAG		59.02
NHX2	**Fwd:** GTCAGCTGGTGTTGGAGTTG	190	59.05
	Rev: GCGCTTCATAACGACTCCAG		59.08

software Image Lab™ 5.2 (Biorad®). Band intensity was estimated by measuring the mean signal intensity of each band, using ImageJ/Fiji (Schindelin et al., 2012). Values were normalized against the relative intensity of tubulin for each situation and relativized against the control.

2.8. Statistical analysis

Each determination was performed on at least three biological replicates ($n \geq 3$). Results were expressed as mean ± standard error of the mean (SEM). After assessing the homogeneity of variances (Brown-Forsythe test), the effects of the two factors [SALT and HEAT] were analysed running a two-way ANOVA (Table S1). Differences between groups were then discriminated by Tukey's post-hoc test. To execute a principal component analysis (PCA), the results obtained for each tested parameter were plotted and the first two components used for biplots. All statistical procedures, along with a Pearson correlation test (Table S2), were performed on GraphPad Prism version 9.5.0 for Windows (GraphPad Software, San Diego, California USA, www.graphpad.com). Data visualization through clustered heatmaps was obtained through the use of the heatmaply package in R.

3. Results

3.1. Specific leaf area (SLA) and cell viability assay

As observed in Fig. 1a, combined stress resulted in smaller leaves than those from the individual conditions, which were equally affected in comparison with the CTL. Concerning cell death, results indicate that no major symptoms were induced regardless of the imposed stress, as no bluish spots could be observed on the leaf surface (Fig. 1a). Although no other severe macroscopic toxicity symptoms were detected, aside from the stunted growth, equally diminished specific leaf area (SLA) was observed for all treatments. This significant reduction in SLA (30–42%) regardless of the stress condition (Fig. 1b) indicates that an increase in leaf mesophyll density and/or thickness occurred independently of the treatment.

3.2. Chlorophylls (a and b) and carotenoids

As can be seen on Fig. 2 and on Table S1, the ANOVA shows a significant effect of both stress factors on photosynthetic pigments. This was constant among both groups of chlorophylls and carotenoids, with a ~24% decrease for HEAT and a 30–38%% for SALT. The COMBINED treatment led to a decrease of ~70% in both photosynthetic pigments.

3.3. Chlorophyll fluorometry

3.3.1. Photochemical efficiency at plant growing light conditions

Results indicate that there was a small yet significant increase (3%) in F_v/F_m in plants grown under the combined treatment (Fig. 3a). Besides, despite the individual stressors negatively affecting $\Phi_{PSII,}$ and rETR (reductions of 8% and 22% for SALT and HEAT, respectively), no differences were found between leaves of COMBINED and CTL (Fig. 3b and c). Lastly, NPQ was increased in all stressed plants (SALT: 193%; HEAT: 103%; COMBINED: 119%) when compared to the CTL (Fig. 3d).

3.3.2. Rapid light curves (RLC)

The plot in Fig. 4 shows the variation of photochemical efficiency of PSII (a), electron transport rate (b), and non-photochemical efficiency

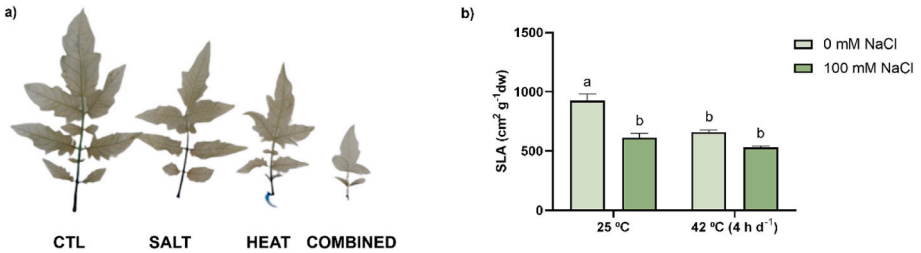

Fig. 1. Cell death (a) and specific leaf area (b) in *Solanum lycopersicum* plants after 3-weeks of growth under daily exposure to 42 °C (4 h) and irrigation with or without 100 mM NaCl. Leaves in (a) are visually representative of each situation. Data are presented as mean ± SEM ($n \geq 3$). Distinct letters above bars indicate significant ($p \leq 0.05$) differences between groups.

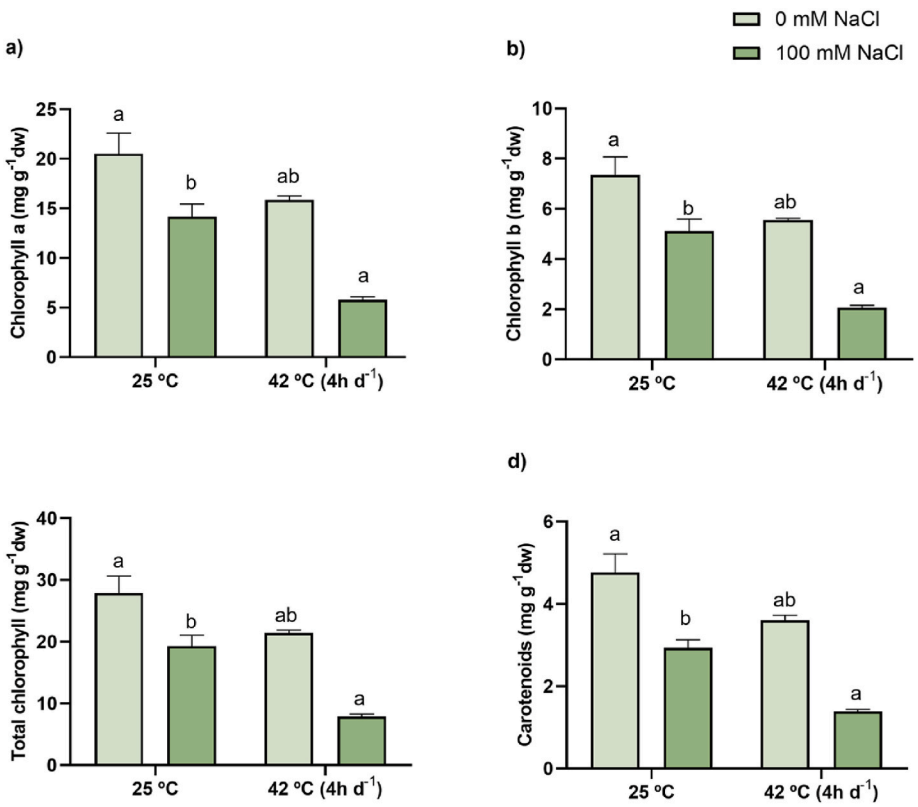

Fig. 2. Chlorophyll *a* (a) and *b* (b), total chlorophyll (c) and carotenoid (d) content of *Solanum lycopersicum* leaves after 3-weeks of growth under daily exposure to 42 °C (4 h) and irrigation with or without 100 mM NaCl. Data are presented as mean ± SEM (n ≥ 3). Distinct letters above bars indicate significant ($p \leq 0.05$) differences between groups.

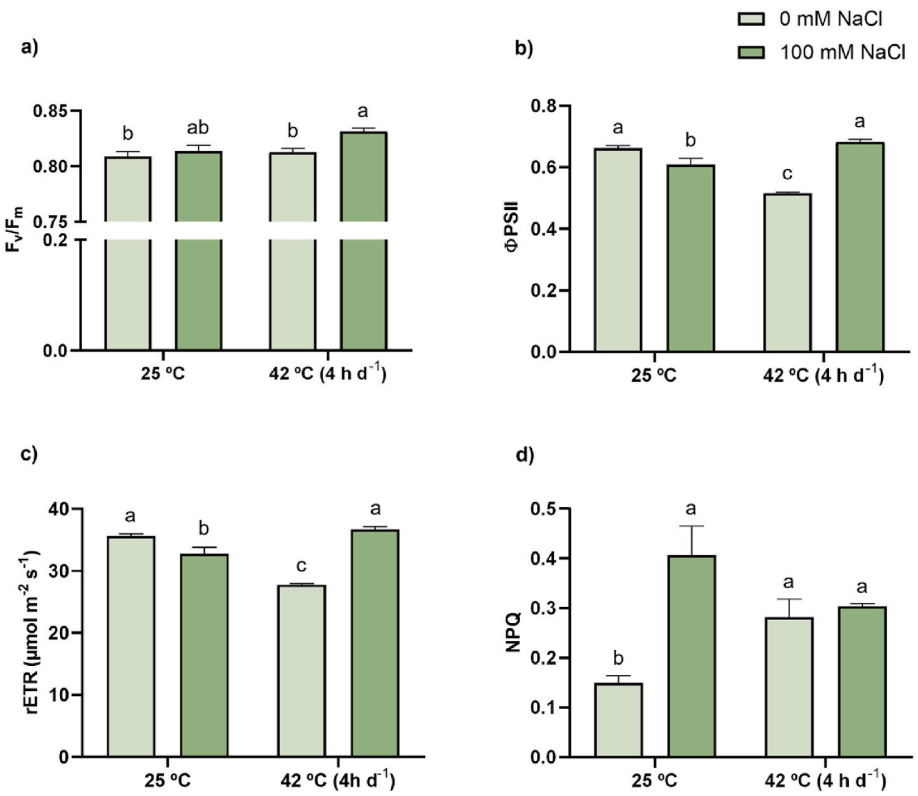

Fig. 3. F_v/F_m (a), Φ_{PSII} (b), rETR (c), and NPQ (d) of *Solanum lycopersicum* leaves after 3-weeks of growth under daily exposure to 42 °C (4 h) and irrigation with or without 100 mM NaCl. Data are presented as mean ± SEM (n ≥ 3). Distinct letters above bars indicate significant ($p \leq 0.05$) differences between groups.

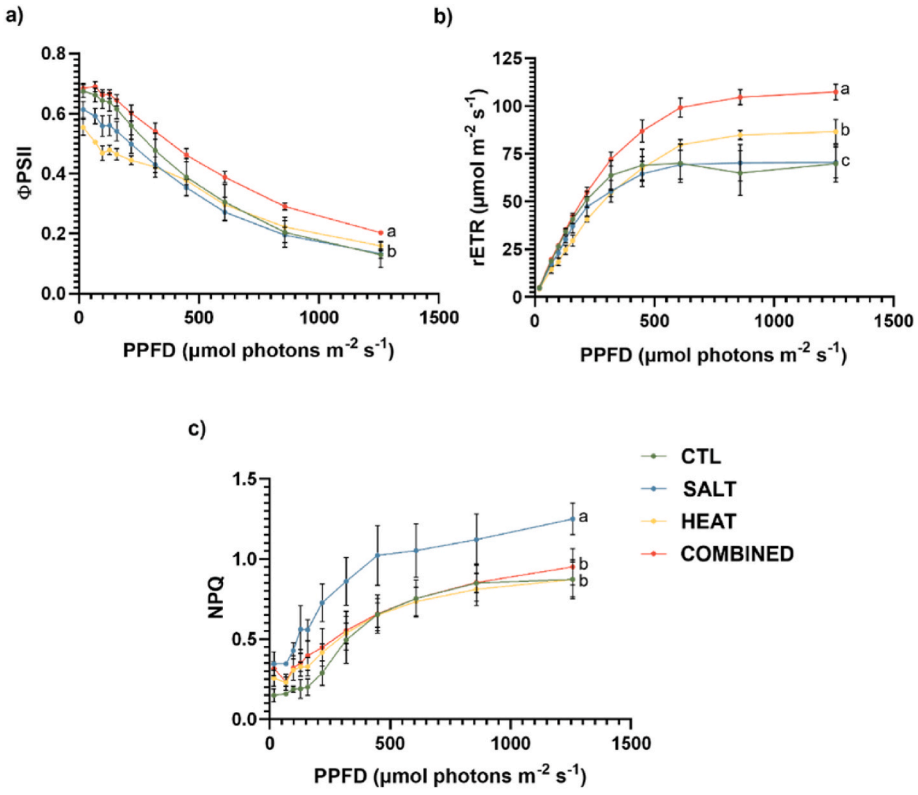

Fig. 4. Φ_{PSII} (a), rETR (b), and NPQ (c) of *Solanum lycopersicum* leaves exposed to PPFD increments after 3-weeks of growth under daily exposure to 42 °C (4 h) and irrigation with or without 100 mM NaCl. Data are presented as mean ± SEM (n ≥ 3). Distinct letters above bars indicate significant ($p \leq 0.05$) differences between groups.

(c) as a function of increasing light intensities in the rapid light curves trials. CTL and SALT appear to saturate at PPFD ~500–600 µmol photons m^{-2} s^{-1}, with the maximum ETR values being around 70 µmol m^{-2} s^{-1}. Contrarily, saturation for COMBINED and HEAT only occurred at the last light step, but while ETR for the former peaked at 80 µmol m^{-2} s^{-1}, COMBINED plants showed maximum values of over 105 µmol m^{-2} s^{-1}.

At low PPFD, all stressed plants were dissipating more light energy by NPQ than the CTL, however, for successive increments in light intensity this difference diminishes, and only plants singly exposed to salinity stress consistently maintained higher NPQ values than CTL (Fig. 4c), which corroborates the results obtained under growth light conditions (Fig. 3 d).

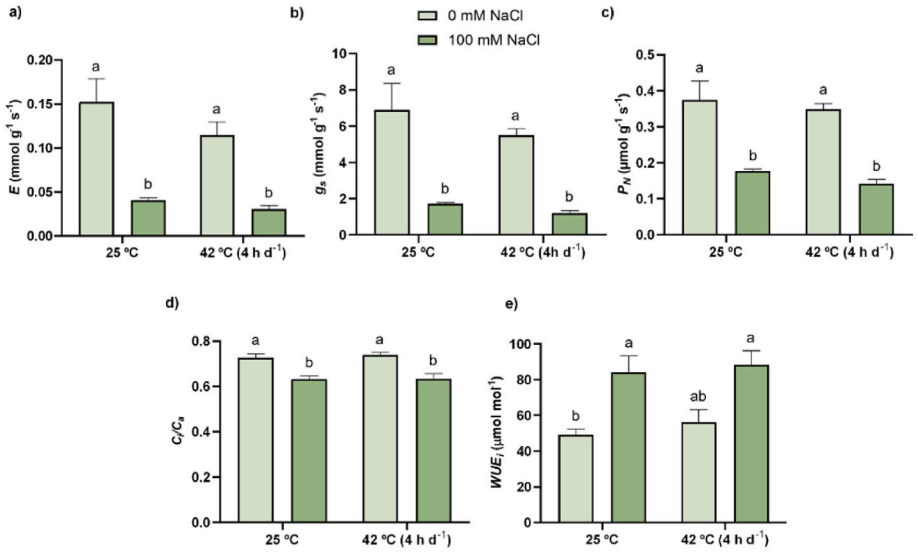

Fig. 5. Transpiration (a), stomatal conductance (b), carbon assimilation (c), C_i/C_a (d), and WUE_i (e) of *Solanum lycopersicum* leaves after 3-weeks of growth under daily exposure to 42 °C (4 h) and irrigation with or without 100 mM NaCl. Data are presented as mean ± SEM (n ≥ 3). Distinct letters above bars indicate significant ($p \leq 0.05$) differences between groups.

3.4. Gas exchange measurements

Regarding gas-exchange parameters (Fig. 5), there is a clear distinction between two groups (CTL and HEAT x SALT and COMBINED). The latter pair of stressed plants exhibited decreased E and g_s (~70–80%; Fig. 5a and b), P_N (~55%, Fig. 5c), and C_i/C_i (14%, Fig. 5d). As expected, an opposite pattern was observed for WUE_i (Fig. 5e), since the reduction caused by these treatments in g_s was higher than in P_N (Fig. 5b and c), with SALT and COMBINED presenting values ~80% higher than those found in CTL plants.

3.5. D1, CP47, RbcS and RbcL gene expression pattern

SALT heavily impacted the transcript accumulation of both PSII-related genes by 85–90% (Fig. 6a and b), while the combination with heat led to a lesser inhibitory response of 55% and 73% for *CP47* and *D1*, respectively, with the ANOVA showing an interaction between HEAT and SALT (Table S1). HEAT plants showed an inhibition of 72% for both genes. Regarding RuBisCO (Fig. 6c and d), *RbcS*, a gene located in the nuclear genome, was identically repressed by both stressors and their combination (40–55% lower than in CTL) but for *RbcL*, located in the chloroplast genome, the lowest transcript accumulation (76% less than CTL) was observed for HEAT treatment. Contrarily, SALT led to the highest accumulation of *RbcL* transcripts, with a 74% increment in relation to the CTL. In combination with HEAT (COMBINED), the accumulation of *RbcL* transcripts decreased in relation to SALT, being statistically similar to the CTL (Fig. 6d).

3.6. Transcriptional regulation of heat and salinity stress-related genes

Data revealed that only HEAT led to an inhibition of *HsfA1* transcription (53%) (Fig. 7a). Regarding *HsfA2*, no differences could be found between the stress conditions and the CTL (Fig. 7b). In Fig. 7c, it can be observed that transcript accumulation for *Hsp70* was strongly increased (about 2.94-fold) under high-temperature treatments (HEAT and COMBINED). On another hand, only the SALT treatment had an effect on the expression of *NHX2* causing a 71% increase in its transcripts (Fig. 7d).

3.7. Western-blotting analysis of D1 and RbcL content

Protein immunoblots analysis, and pixel-based quantification of band intensity (normalized against the tubulin band intensity), indicated that the content of D1 protein (~35 kDa) decreased under salt exposure, individually (67% decrease) and especially in combination with heat (81% decrease), and was slightly less abundant in HEAT (decrease of 25%) as well (Fig. 8a). Contrarily, regarding RbcL (~50 kDa), all stress conditions led to a higher accumulation of this protein (1.675- and 2.99-fold increase in SALT and HEAT, respectively), especially in the combined treatment (4.48-fold) (Fig. 8b).

3.8. Principal component analysis (PCA) and clustered heatmap

A principal component analysis was performed to find correlations between distinct groups/conditions and all evaluated endpoints (Fig. 9). Also, a heatmap was constructed from these results to better analyse and summarize the main outputs (Fig. 10). Regarding the PCA, more than 72% of the total variance was explained by the two main components, with the first one explaining 51.92% and the second one 20.24%. As can be observed in Fig. 9, CTL and HEAT appeared to be distant from each other (respectively in the 2nd and 3rd quadrants) and from the other two treatments, SALT and COMBINED, that showed high proximity, appearing both in the 1st quadrant. This separation between groups can also be perceived on the clustered heatmap (Fig. 10), where both salt treatments are mostly associated with decreased photosynthetic pigments, gas-exchange parameters, and the expression of genes coding for PSII crucial proteins (CP47 and D1) as well as protein levels of D1. Furthermore, both employed approaches highlighted that CTL plants were characterized by a high expression of photosynthesis-related genes and an enhanced content of photosynthetic pigments, as well as improved P_N, g_s, and E. Contrastingly, combined stress differed from all other treatments by a very high decrease of chlorophyll and carotenoids and an increment in F_v/F_m and rETR and Φ_{PSII}, the latter especially in the RLC trial.

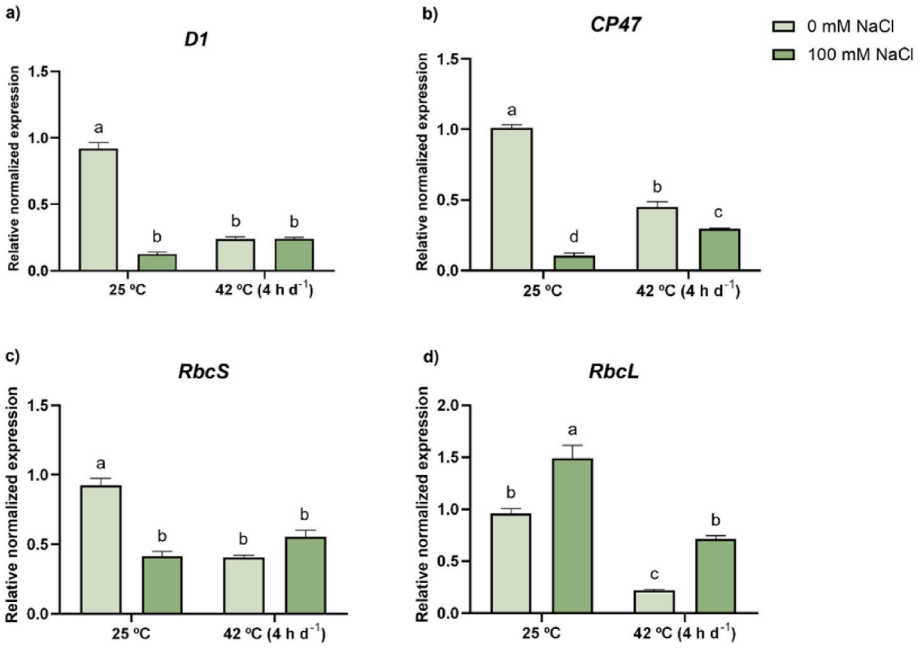

Fig. 6. Transcript accumulation of *D1* (a), *CP47* (b), *RbcS* (c), and *RbcL* (d) of *Solanum lycopersicum* leaves after 3-weeks of growth under daily exposure to 42 °C (4 h) and irrigation with or without 100 mM NaCl. Data are presented as mean ± SEM ($n \geq 3$). Distinct letters above bars indicate significant ($p \leq 0.05$) differences between groups.

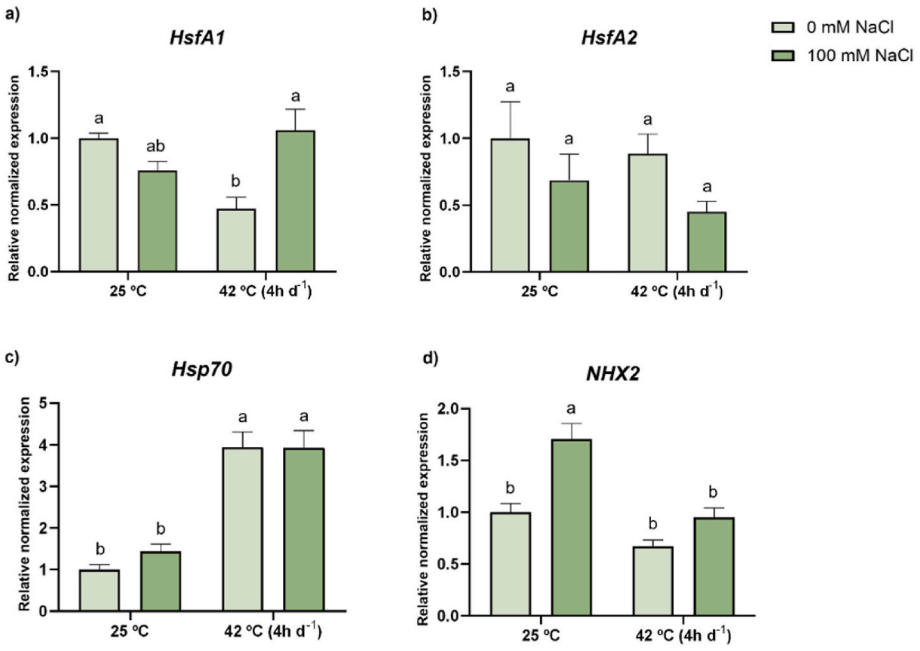

Fig. 7. Transcript accumulation of *HsfA1* (a), *HsfA 2* (b), *Hsp70* (c), and *NHX2* (d) of *Solanum lycopersicum* leaves after 3-weeks of growth under daily exposure to 42 °C (4 h) and irrigation with or without 100 mM NaCl. Data are presented as mean ± SEM (n ≥ 3). Distinct letters above bars indicate significant ($p \leq 0.05$) differences between groups.

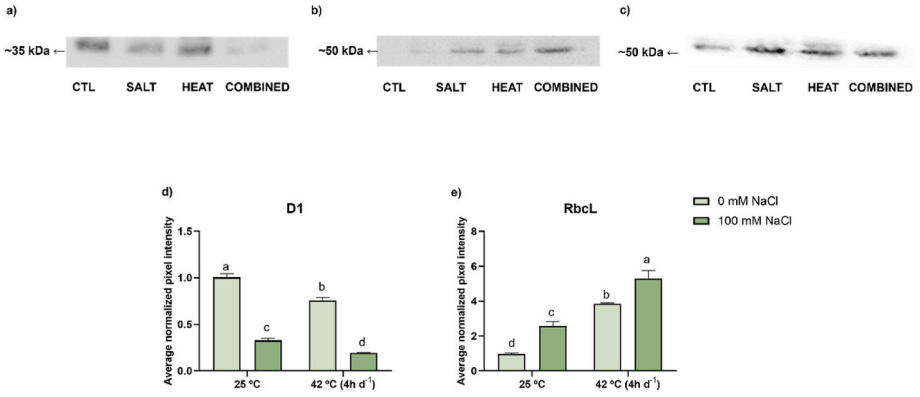

Fig. 8. Immunoblot analyses of D1 (AS05 084, Agrisera, Sweden) (a) and RbcL (AS03 037, Agrisera, Sweden) (b) protein abundance in *Solanum lycopersicum* leaves after 3-weeks of growth under daily exposure to 42 °C (4 h) and irrigation with/without 100 mM NaCl. Tubulin (AS10 680, Agrisera, Sweden) (c) was used as a reference protein. Pixel intensity was calculated by normalization against the reference protein and values were normalized against the control for D1 (d) and RbcL (e). Data are presented as mean ± SEM (n ≥ 3). Distinct letters above bars indicate significant ($p \leq 0.05$) differences between groups.

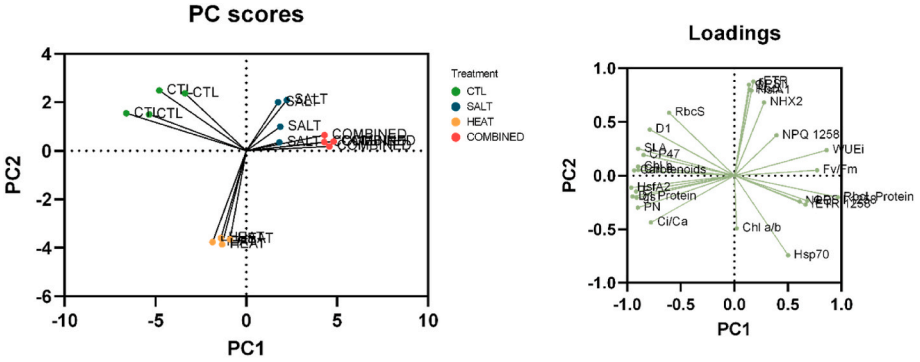

Fig. 9. Biplot-based PCA elucidating the differential response of Solanum *lycopersicum* plants after 3-weeks of growth under daily exposure to 42 °C (4 h) and irrigation with or without 100 mM NaCl.

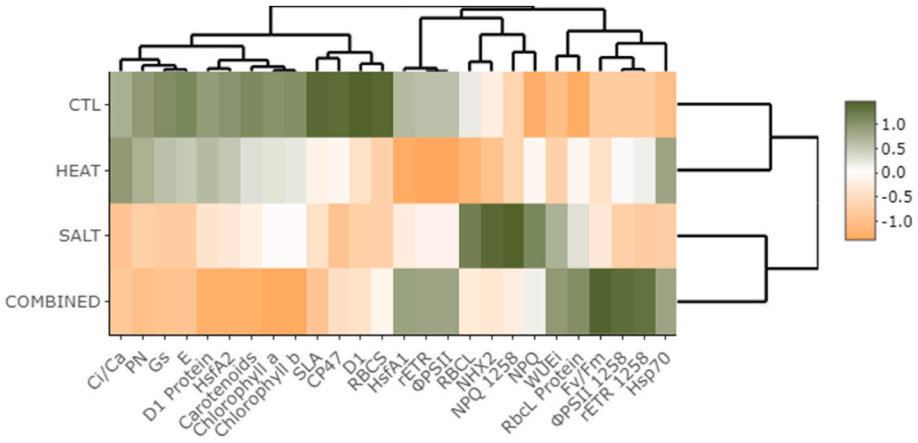

Fig. 10. Clustered heatmap, elucidating the differential response on the performance of *Solanum lycopersicum* plants after 3-weeks of growth under daily exposure to 42 °C (4 h) and irrigation with or without 100 mM NaCl. The mean values of the numerous parameters obtained in this study were normalized and clustered. The color scale displays the intensity of normalized mean values of distinct parameters.

4. Discussion

Together with drought, the rising heat waves and increased salinization are two of the most impactant abiotic stresses nowadays. Thus, as a follow-up to our previous work on the regulation of the plants' redox status (Sousa et al., 2022), this study aimed to unravel the response of cherry tomato plants to the combination of heat and salt stresses in terms of photosynthetic performance and cell viability.

4.1. The combination of stresses was the most impactful treatment in plant performance, despite all treatments equally diminishing SLA

Tomato plants exposed to either salt or heat present reduced organ elongation and biomass, with the co-exposure to both stresses leading to a more severe effect (Sousa et al., 2022). This damage was associated with a disturbed ionic balance, with an increased sodium accumulation leading to high phytotoxicity (Sousa et al., 2022). The present results show that these negative effects also expand in terms of leaf area and mesophyll structure, which was confirmed by the impact of the different treatments on SLA. Despite other works showing the opposite, some reports suggest that salt stress can lead to thicker leaf lamina, which can result from bigger mesophyll cells or increased cell layers (Bayuelo--Jiménez et al., 2012). Also, the results of Bayuelo-Jiménez et al. (2012) showed that *Phaseolus* species exposed to increasing NaCl levels presented lower SLA, which in turn, in salt-tolerant genotypes, was suggested to be a tolerance mechanism. Since salt-induced stomata closure can lead to decreased carbon availability, plants presenting thicker mesophylls might have increased internal surface area for CO_2 absorption, counteracting limited carbon assimilation. Thus, the reduction in SLA could be a way to mitigate the stomatal limitations of photosynthesis and, hence, plant growth. Moreover, previous works (Poorter and Garnier, 2007) comparing species with contrasting SLA values, showed that, under stress conditions, a lower SLA is correlated with higher nutrient retention and protection from dehydration. In this sense, the reduction of SLA herein observed can indicate a possible defensive trait, mostly when considering SALT and COMBINED.

Regarding HEAT, a different strategy can be hypothesized, since irrigation was not limiting and previous reports show that the reduced biomass was not related to nutrient imbalances in plants exposed to these conditions (Sousa et al., 2022). Knight and Ackerly (2003) reported that plants with lower SLA presented increased thermotolerance, with this higher mesophyll density being coupled with a higher HSP content in the chloroplast and an enhanced ETR recovery after heat stress. Curiously, our results only agree with this assessment when plants were submitted to the joint effect of both heat and salinity. Nonetheless, both heat-related treatments presented higher rETR at increasing light intensities, which might indicate the enhancement of protective strategies.

In what concerns the combined stress, it is possible to see that leaf size was severely reduced in comparison with the individual stresses, being directly related to the decreased height and biomass previously observed by our research group (Sousa et al., 2022). We had previously hypothesized that this synergistic effect between stressors in plant growth could be related to salinity negatively influencing the transpiration rate, thus increasing the susceptibility to heat stress (Sousa et al., 2022). However, in terms of photosynthetic performance assessed by PAM fluorometry and gas-exchange parameters, plants subjected to combined stressors were not more affected than those subjected to individual stressors. Therefore, the severely reduced plant growth observed can be ascribed mainly to the mobilization of resources for defense pathways (Sousa et al., 2022) or the negative impacts of these stress factors in other important processes, such as cell expansion and division.

Furthermore, even though salinity (Parihar et al., 2015) and moderate heat stress (Hassan et al., 2021; Wahid et al., 2007) commonly lead to cell death, Evans Blue dye was not able to cross the membranes indicating that these stressors did not significantly affect cell viability. Indeed, previous results (Sousa et al., 2022) have shown that, at least in these conditions, tomato plants exposed to salt and/or heat, did not present increased lipid peroxidation, with these results being related to an efficient antioxidant machinery, where proline had a prominent role since this metabolite is heavily associated with membrane stability (Spormann et al., 2023). Moreover, another work (Banu et al., 2009) demonstrated the importance of proline in reducing cell damage in salt-stressed (50–200 mM NaCl) tobacco.

4.2. Heat and salt combination impacts the transcriptional and biochemical control of photosynthetic players, but without major effects on overall yield

The initial step in the photosynthetic machinery is the absorption of light energy by the photosynthetic pigments chlorophylls and carotenoids. Although very important, they are also very susceptible to stress (Singh et al., 2018), with heat and salt being able to interfere with the production of chlorophyll precursors and the activity of several important players in the biosynthetic pathways of chlorophylls and carotenoids (Ashraf and Harris, 2013; Santos, 2004; Ann et al., 2011; Maurya et al., 2015). Accordingly, the results herein obtained show that these stressors impacted either the production or degradation of both sets of pigments, leading to a reduction in their levels. Moreover, these effects

were mostly perceived in the co-exposure scenario, severely lowering chlorophyll and carotenoid content, which can indicate a more pronounced impact on common pathways and/or a synergistic effect of both stressors on different players involved in pigment synthesis and degradation. Moreover, while tomato plants exposed to salt alone did not exhibit any Mg^{2+} deficiency, there was a depletion of this important chlorophyll component in plants subjected to both stressors (Sousa et al., 2022), which might also be related with the severity of the combined stress in chlorophyll content.

Upon photon absorption in the reaction centres of PSII and PSI, excited chlorophyll molecules transfer their energy to other chlorophyll molecules in the form of heat or light (known as fluorescence). This process occurs in the PSII, aided by light harvesting complexes (LHCII), which are associated with the PSII core complex, that comprise D1 and CP47, a core reaction centre protein and an antenna protein, respectively (Derks et al., 2015). As such, these proteins are key to a proper photosynthetic process and the entire ETC can be compromised if these proteins are damaged or their gene expression is altered, which is a common consequence of the exposure to adverse conditions (Pospíšil and Prasad, 2014). Indeed, transcript accumulation for the genes encoding both these proteins were heavily decreased by all treatments in the present study. Salinity stress often results in a diminished content of the D1 protein, as registered in the present study in both saline treatments, and in tomato exposed to 150 and 200 mM NaCl (Yin et al., 2019; Zhou et al., 2016; Zhang et al., 2012; Sun et al., 2010). This occurs most likely as a consequence of the accumulation of FtsH-like proteins, which are involved in D1 degradation (Kirchhoff, 2019), along with the impairment of its *de novo* synthesis. Additionally, there is also a decrease in polypeptide accumulation when plants were exposed only to heat, which is in accordance with the suppressed gene expression and the existing literature (Zahra et al., 2023). Moreover, considering the harsher effect of the combined treatment, when compared to plants exposed only to salt stress, it seems that heat may be playing a significant role concerning D1 content. Nonetheless, to gain a further insight into the mechanisms governing the photosynthetic reaction centre, further studies should be conducted with a focus on FtsH, as well as the sigma factor, which modulate chloroplast transcription throughout plant development and after exposure to environmental constraints (Kanamaru and Tanaka, 2004; Yoshioka and Yamamoto, 2011).

Briefly, all stress treatments led to a decline in photosynthetic pigments, especially the combined stress, and resulted in the inhibition of the expression of *CP47* and *D1*, which, consequently, culminated in the diminished content of the D1 protein. Since the ETC may be compromised, this study investigated how these plants responded to increasing light intensities (Fig. 4). HEAT and COMBINED portrayed greater ETR_{max}, while salinity individually led to the highest NPQ by conveying more exciting energy to non-photochemical mechanisms (Figs. 3 and 4), which is in accordance with the lower ETR_{max} values for SALT (Fig. 4). In fact, through the dissipation of excess light energy as heat, ROS overproduction and the photodamage of PSII can be avoided, making this a possible tolerance mechanism. On the other hand, heat exposure, individually or in combination with salt, seems to induce defensive pathways (HSPs, increased abundance of RuBisCO, or boosted antioxidant system), minimizing the effects of the stressors on photosynthesis. Nonetheless, and as also observed by Olmo et al. (2014) and Soares et al. (2020), the reduction in SLA (higher amount of cells per leaf area and, consequently, increased PSII reaction centres in the portion of the leaf analysed by PAM) may not fully explain the photosynthetic potential at the whole plant level, especially given the morphological differences between groups. This would be in agreement with the increase in NPQ (dissipated energy), which could be noticed in plants from all treatments and that has also been reported in heat- (Jahan et al., 2021) and salt-stressed plants (Zribi et al., 2009). Still, it is curious that, at growth-light conditions, the individual stressors affected Φ_{PSII}, and consequently rETR, more than the combined stress, possibly indicating a convergence of protective pathways to prevent more severe effects. Lastly, it is important to keep in mind that, although PSII is considered to be more sensitive to the impacts of stress than PSI, the latter can also be disrupted, leading to high impacts on the photosynthetic apparatus. As such, follow-up studies focusing on the connection between both photosystems and the photochemical stage of photosynthesis can grant important insight regarding the impacts of these stress conditions on plant performance.

4.3. Salt stress, regardless of heat, was the main factor affecting gas-exchange parameters

Understanding how RuBisCO behaves under stress conditions is pivotal to pinpoint the photosynthetic responses of plants facing unfavorable environments, since this enzyme is known to be sensitive to different abiotic stress factors (Parihar et al., 2015; Mathur et al., 2014). This highly important and abundant protein consists of small (RbcS) and large (RbcL) subunits, coded by nuclear and chloroplastidial genes, respectively (Spreitzer and Salvucci, 2002). Here, gene expression of both *RbcS* and *RbcL* was inhibited in heat-stressed plants, a result alike those documented in *S. lycopersicum* seedlings after a 24 h exposure to 42 °C (Jahan et al., 2021). Interestingly, this did not translate into lower CO_2 assimilation. This can be related to the recovery period between heat treatments, as some chloroplast genes, such as *RbcL*, can be severely reduced after heat treatment but then recover to normal levels (Danilova et al., 2018), and this equilibrium possibly being sufficient to not affect P_N, with this maintenance of P_N also being shown in wheat (Kreslavski et al., 2008). This, along the lack of water limitation, is also related with the unchanged stomatal conductance (g_s) and transpiration (E), since heat-related water stress is linked with stomata closure (Hassan et al., 2020). Curiously, even though the expression of both *RbcS and RbcL* was severely repressed, immunoblot analysis for the RbcL protein showed an increased content. Since the biosynthesis of this protein is not being stimulated under heat stress, this may be related to a diminished degradation. Indeed, it has been suggested that high concentrations of ROS generated under stress conditions impose modifications on RbcL, to favor its degradation by proteases (Desimone et al., 1996). This is most likely triggered by an accumulation of H_2O_2 (Marín-Navarro and Moreno, 2003), which was not seen in plants exposed to heat in our previous work (Sousa et al., 2022). A similar rationale can be applied to COMBINED, although here there was a clear decrease in CO_2 assimilation, due to the interaction with a saline environment. Indeed, our results clearly indicate that the effects of heat and salt co-exposure are majorly deriving from the salinity toxicity, as there is a clear separation between salt-stressed and non salt-stressed plants (Fig. 5). In fact, salt (alone or in combination) led to reduced water uptake in shoots (Sousa et al., 2022) and decreased g_s to prevent water losses, diminishing transpiration (E), carbon assimilation (P_N), and intercellular CO_2, [0.8–0.9 correlation index (Table S2)] and enhancing WUE_i, a result similar to those obtained by Lopez-Delacalle et al. (2021) in the salinity treatment. Despite these effects on C assimilation, *RbcL* was either down-regulated (SALT) or unchanged (COMBINED), respectively. Commonly, reduced P_N is ascribed to a carboxylation efficiency and inhibited RuBisCO activity (ElSayed et al., 2021), but alterations in P_N can also result from changes in g_s (von Caemmerer and Farquhar, 1981). In fact, intercellular CO_2 concentration was negatively affected by both salt treatments, despite *RbcL* accumulation, which could be caused by the lower g_s [correlation index of 0.861 (Table S2)] and not related to changes in *RbcL* expression [correlation index of −0.517 (Table S2)].

4.4. Heat exposure modulated the heat shock response but negatively affected salt-induced ionic balance pathways

When exposed to situations of heat stress, tomato plants take advantage of a complex defense mechanism, triggered by the tomato heat stress transcription factor (TF) A1 (*SlHsfA1*). As this TF is upregulated, so are others, including *HsfA2*, which allows improved signaling

pathways and, consequently, increased thermotolerance (Fragkostefanakis et al., 2019; Khan et al., 2020; Yu et al., 2019). Curiously, our results portray a contrasting response, with plants exposed to heat stress, either individually or in combination, showing a lower or unaltered transcript accumulation for both these genes. Nonetheless, it is worth noting that, although in the present study plants were exposed daily to high temperatures, leading to decreased growth performance (Sousa et al., 2022), the heat treatment was provided in a short period with a 20 h recovery. Indeed, Rao et al. (2021) showed that when tomato plants were exposed to 45 °C for 2 h, there was a sharp upregulation of *HsfA1* and *HsfA2*, but 24 h after heat exposure, transcript levels were down-regulated to levels below control, similar to the results herein presented. Hahn et al. (2011) and Rao et al. (2021) have reported a model where, under optimum conditions, HsfA1 is inactivated by the interaction between two molecular chaperones – Hsp70 and Hsp90 – and, when heat stress is applied, these chaperones function in preventing the stress-induced loss of stability or function of damaged proteins. As such, HsfA1 is no longer inactive, thus activating other genes related to stress memory and repair mechanisms, which remain upregulated in the recovery phase (Rao et al., 2021). Afterwards, the increase in free Hsp70 and Hsp90 leads back to the inactivation of the class A heat shock TF. Actually, our results point towards increased *Hsp70* in heat stress, with this being negatively correlated with the expression of *HsfA1* and *HsfA2* (Table S2). Taking all of this into consideration, it is possible that when heat stress is applied and protein stability is in danger, there is an urgent need for the synthesis of molecular chaperones to ensure proper plant performance. Then, as the recovery stage sets in and the memory and repair players are already activated and performing their function, this high increase in *Hsp70* maintains the inactivation of the class A TF, possibly as an energy-saving mechanism, as hypothesized by Rao et al. (2021). Even though not much is known regarding the combined action of heat and salt, this higher increase in *Hsp70* transcripts when heat is applied in combination with another stressor has already been reported for drought in tomato (Raja et al., 2020) and maize (Hu et al., 2010), highlighting the implications of climate change-related aggravation on plant physiology, severely affecting protein stability.

Controlling nutrient balance and ionic toxicity is also a major part of the plant defense mechanism against challenges imposed by climate change, especially when grown under highly saline environments. In our previous record, tomato plants exposed to the combined stresses accumulated less K^+, Ca^{2+}, and Mg^{2+} and much more Na^+ than when only salt was applied (Sousa et al., 2022). Thus, it was hypothesized that this nutrient imbalance would repress the Salt Overly Sensitive (SOS) pathway, which works by allowing the efflux of Na^+ (Ji et al., 2013). This removal of excess Na from the cytoplasm is highly associated with tonoplast Na^+/H^+ antiporters such as NHX2 (Ji et al., 2013). The results herein obtained show that whereas plants treated only with salt have increased transcript accumulation of *NHX2*, correlating with less stunted growth, no changes could be noticed when plants were exposed to combined stress. As such, since the SOS pathway is mediated by Ca^+, this deficiency can limit the plant's ability to maintain a proper ionic balance in the cytoplasm, ultimately leading to ionic toxicity and the inability of the plant to thrive in this environment. Similarly, and although there is not much knowledge regarding the mechanisms of ion transport, especially in combined stress, maize plants exposed to the combined action of the salt (150 mM NaCl) and boron also showed the induction of *NHX2* and *SOS1* when only salt was applied alone (Huanca-Mamani et al., 2018).

5. Conclusion

With the results herein gathered, and by implementing an environmentally-relevant approach, an insightful picture around the major impacts of combined salt and heat stress in tomato plants' photosynthetic metabolism was achieved. Altogether, data revealed that both stresses resulted in lower content of chlorophylls and carotenoids, decreased SLA, and the inhibition of photosynthesis-related genes (*CP47*, *D1,* and *RbcS*). However, while salt had a predominantly negative effect on *in vivo* gas exchange endpoints, PSII appeared to be more susceptible to heat than to the other conditions, at least under growing-light conditions. Despite that, and possibly due to improved defensive pathways (such as the HSP response), plants subjected to heat (individually or combined) appear to be better adapted to increasing light intensities. On a general note, when observing the PCA (Fig. 9) and heatmap (Fig. 10), it can be concluded that, despite their slightly different profiles, SALT and COMBINED were plotted very closely, thus the effects of the co-exposure appear to be mostly a result of salt exposure. Here, the main differences between these treatments are the above-mentioned less affected chlorophyll fluorescence endpoints in COMBINED, at growing and high light, as well as the perceived lower efficiency of the nutrient balance pathways (*NHX2*). Moreover, the combined situation was plotted separately from CTL and HEAT, mostly due to the former having increased values of F_v/F_m, WUE_i, and NPQ and severely lower levels of photosynthetic pigments, as well as decreased E, P_N, g_s, and C_i/C_a. Overall, the combined salt and heat stress does not appear to cause more damage on photosynthetic performance than the individual stressors.

Funding

The work here presented was partially supported by national funds through the Foundation for Science and Technology (FCT), within UIDB/05748/2020 and UIDP/05748/2020 (GreenUPorto), UIDB/04050/2020 (CBMA), UIDB/50006/2020 (LAQV-REQUIMTE) and UIDB/04033/2020 (CITAB). The authors also recognize the support by the I&D project "AgriFood XXI", ref. NORTE-01-0145-FEDER-000041, co-financed by the European Regional Development Fund (FEDER), through NORTE 2020 (Northern Regional Operational Program, 2014/2020). B. Sousa and D. Moreira also acknowledge FCT for providing PhD student grants (BS: 2020/07826/BD; DM: SFRH/BD/143557/2019).

Author contribution

Francisca Rodrigues - Formal analysis, Investigation, Writing – original draft, Writing – review & editing. Bruno Sousa – Conceptualization, Formal analysis, Investigation, Writing – original draft, Writing – review & editing. Cristiano Soares – Investigation, Writing – review & editing. Diana Moreira – Investigation. Cláudia Pereira – Resources, Investigation, Writing – review & editing. José Moutinho-Pereira – Resources, Investigation, Writing – review & editing. Ana Cunha – Resources, Supervision, Writing – review & editing. Fernanda Fidalgo – Conceptualization, Project administration, Funding acquisition, Resources, Supervision, Writing – review & editing.

Declaration of competing interest

The authors declare that they have no known competing financial interests or personal relationships that could have appeared to influence the work reported in this paper.

Data availability

Data will be made available on request.

Appendix A. Supplementary data

Supplementary data to this article can be found online at https://doi.org/10.1016/j.plaphy.2023.108270.

References

Al-Whaibi, M.H., 2011. Plant heat-shock proteins: a mini review. J. King Saud Univ. Sci. 23, 139–150. https://doi.org/10.1016/j.jksus.2010.06.022.

Ann, B.M., Devesh, S., Gothandam, K.M., 2011. Effect of salt stress on expression of carotenoid pathway genes in tomato. J. Stress Physiol. Biochem. 7.

Ashraf, M., Harris, P.J.C., 2013. Photosynthesis under stressful environments: an overview. Photosynthetica 51, 163–190. https://doi.org/10.1007/s11099-013-0021-6.

Ayers, R.S., Westcot, D.W., 1985. Water Quality for Agriculture. Rome.

Banu, M.N.A., Hoque, M.A., Watanabe-Sugimoto, M., Matsuoka, K., Nakamura, Y., Shimoishi, Y., et al., 2009. Proline and glycinebetaine induce antioxidant defense gene expression and suppress cell death in cultured tobacco cells under salt stress. J. Plant Physiol. 166, 146–156. https://doi.org/10.1016/j.jplph.2008.03.002.

Bayuelo-Jiménez, J.S., Jasso-Plata, N., Ochoa, I., 2012. Growth and physiological responses of *Phaseolus* species to salinity stress, 2012 Int J Agron, 527673. https://doi.org/10.1155/2012/527673.

Bradford, M.M., 1976. A rapid and sensitive method for the quantitation of microgram quantities of protein utilizing the principle of protein-dye binding. Anal. Biochem. 72, 248–254. https://doi.org/10.1016/0003-2697(76)90527-3.

Carvalho, D., Cardoso Pereira, S., Rocha, A., 2021. Future surface temperature changes for the Iberian Peninsula according to EURO-CORDEX climate projections. Clim. Dynam. 56, 123–138. https://doi.org/10.1007/s00382-020-05472-3.

Daliakopoulos, I.N., Tsanis, I.K., Koutroulis, A., Kourgialas, N.N., Varouchakis, A.E., Karatzas, G.P., et al., 2016. The threat of soil salinity: a European scale review. Sci. Total Environ. 573, 727–739. https://doi.org/10.1016/j.scitotenv.2016.08.177.

Danilova, M.N., Kudryakova, N.V., Andreeva, A.A., Doroshenko, A.S., Pojidaeva, E.S., Kusnetsov, V.V., 2018. Differential impact of heat stress on the expression of chloroplast-encoded genes. Plant Physiol. Biochem. 129, 90–100. https://doi.org/10.1016/j.plaphy.2018.05.023.

Derks, A., Schaven, K., Bruce, D., 2015. Diverse mechanisms for photoprotection in photosynthesis. Dynamic regulation of photosystem II excitation in response to rapid environmental change. Biochim. Biophys. Acta Bioenerg. 1847, 468–485. https://doi.org/10.1016/j.bbabio.2015.02.008.

Desimone, M., Henke, A., Wagner, E., 1996. Oxidative stress induces partial degradation of the large subunit of ribulose-1,5-bisphosphate carboxylase/oxygenase in isolated chloroplasts of barley. Plant Physiol. 111, 789–796. https://doi.org/10.1104/pp.111.3.789.

ElSayed, A.I., Rafudeen, M.S., Gomaa, A.M., Hasanuzzaman, M., 2021. Exogenous melatonin enhances the reactive oxygen species metabolism, antioxidant defense-related gene expression, and photosynthetic capacity of *Phaseolus vulgaris* L. to confer salt stress tolerance. Physiol. Plantarum 173, 1369–1381. https://doi.org/10.1111/ppl.13372.

Eurostat. Crop production in national humidity 2021. https://ec.europa.eu/eurostat/databrowser/view/APRO_CPNH1__custom_5535914/default/table?lang=en, 25.3.23.

Fragkostefanakis, S., Simm, S., El-Shershaby, A., Hu, Y., Bublak, D., Mesihovic, A., et al., 2019. The repressor and co-activator HsfB1 regulates the major heat stress transcription factors in tomato. Plant Cell Environ. 42, 874–890. https://doi.org/10.1111/pce.13434.

Gamborg, O.L., Miller, R.A., Ojima, K., 1968. Nutrient requirements of suspension cultures of soybean root cells. Exp. Cell Res. 50, 151–158. https://doi.org/10.1016/0014-4827(68)90403-5.

Genty, B., Briantais, J.M., Baker, N.R., 1989. The relationship between the quantum yield of photosynthetic electron transport and quenching of chlorophyll fluorescence. Biochim. Biophys. Acta Gen. Subj. 990, 87–92. https://doi.org/10.1016/S0304-4165(89)80016-9.

Haddeland, I., Heinke, J., Biemans, H., Eisner, S., Flörke, M., Hanasaki, N., et al., 2014. Global water resources affected by human interventions and climate change. Proc. Natl. Acad. Sci. USA 111, 3251–3256. https://doi.org/10.1073/pnas.1222475110.

Hahn, A., Bublak, D., Schleiff, E., Scharf, K.D., 2011. Crosstalk between Hsp90 and Hsp70 chaperones and heat stress transcription factors in tomato. Plant Cell 23, 741–755. https://doi.org/10.1105/tpc.110.076018.

Hassan, M.U., Chattha, M.U., Khan, I., Chattha, M.B., Barbanti, L., Aamer, M., et al., 2020. Heat stress in cultivated plants: nature, impact, mechanisms, and mitigation strategies—a review. Plant Biosyst Int J Deal with All Asp Plant Biol 1–24. https://doi.org/10.1080/11263504.2020.1727987.

Hassan, M.U., Chattha, M.U., Khan, I., Chattha, M.B., Barbanti, L., Aamer, M., et al., 2021. Heat stress in cultivated plants: nature, impact, mechanisms, and mitigation strategies—a review. Plant Biosyst - An Int J Deal with All Asp Plant Biol 155, 211–234. https://doi.org/10.1080/11263504.2020.1727987.

Hu, X., Liu, R., Li, Y., Wang, W., Tai, F., Xue, R., et al., 2010. Heat shock protein 70 regulates the abscisic acid-induced antioxidant response of maize to combined drought and heat stress. Plant Growth Regul. 60, 225–235. https://doi.org/10.1007/s10725-009-9436-2.

Huanca-Mamani, W., Ortiz, M.V., Cárdenas-Ninasivincha, S., Acosta-Garcia, G., Bastías, E., 2018. Gene expression analysis in response to combined salt and boron (B) stresses in a tolerant maize landrace. Plant Omics 11, 80–88. https://doi.org/10.21475/poj.11.02.18.pne1144.

IPCC, 2021. Climate Change 2021: the Physical Science Basis. Contribution of Working Group I to the Sixth Assessment Report of the Intergovernmental Panel on Climate Change. Cambridge University Press.

Jahan, M.S., Guo, S., Sun, J., Shu, S., Wang, Y., El-Yazied, A.A., et al., 2021. Melatonin-mediated photosynthetic performance of tomato seedlings under high-temperature stress. Plant Physiol. Biochem. 167, 309–320. https://doi.org/10.1016/j.plaphy.2021.08.002.

Ji, H., Pardo, J.M., Batelli, G., Van Oosten, M.J., Bressan, R.A., Li, X., 2013. The salt overly sensitive (SOS) pathway: established and emerging roles. Mol. Plant 6, 275–286. https://doi.org/10.1093/mp/sst017.

Kanamaru, K., Tanaka, K., 2004. Roles of chloroplast RNA polymerase sigma factors in chloroplast development and stress response in higher plants. Biosci. Biotechnol. Biochem. 68, 2215–2223. https://doi.org/10.1271/bbb.68.2215.

Khan, A., Khan, A.L., Imran, M., Asaf, S., Kim, Y.H., Bilal, S., et al., 2020. Silicon-induced thermotolerance in *Solanum lycopersicum* L. via activation of antioxidant system, heat shock proteins, and endogenous phytohormones. BMC Plant Biol. 20, 248. https://doi.org/10.1186/s12870-020-02456-7.

Kirchhoff, H., 2019. Chloroplast ultrastructure in plants. New Phytol. 223, 565–574. https://doi.org/10.1111/nph.15730.

Kitajima, M., Butler, W.L., 1975. Quenching of chlorophyll fluorescence and primary photochemistry in chloroplasts by dibromothymoquinone. Biochim. Biophys. Acta Bioenerg. 376, 105–115. https://doi.org/10.1016/0005-2728(75)90209-1.

Knight, C.A., Ackerly, D.D., 2003. Evolution and plasticity of photosynthetic thermal tolerance, specific leaf area and leaf size: congeneric species from desert and coastal environments. New Phytol. 160, 337–347. https://doi.org/10.1046/j.1469-8137.2003.00880.x.

Koutroulis, A.G., Tsanis, I.K., Daliakopoulos, I.N., Jacob, D., 2013. Impact of climate change on water resources status: a case study for Crete Island, Greece. J. Hydrol. 479, 146–158. https://doi.org/10.1016/j.jhydrol.2012.11.055.

Kreslavski, V., Tatarinzev, N., Shabnova, N., Semenova, G., Kosobryukhov, A., 2008. Characterization of the nature of photosynthetic recovery of wheat seedlings from short-term dark heat exposures and analysis of the mode of acclimation to different light intensities. J. Plant Physiol. 165, 1592–1600. https://doi.org/10.1016/j.jplph.2007.12.011.

Laemmli, U.K., 1970. Cleavage of structural proteins during the assembly of the head of bacteriophage T4. Nature 227, 680–685. https://doi.org/10.1038/227680a0.

Lichtenthaler, H.K., 1987. [34] Chlorophylls and carotenoids: pigments of photosynthetic biomembranes. Elsevier Methods Enzymol. 148, 350–382. https://doi.org/10.1016/0076-6879(87)48036-1.

Livak, K.J., Schmittgen, T.D., 2001. Analysis of relative gene expression data using real-time quantitative PCR and the $2^{-\Delta\Delta CT}$ method. Methods 25, 402–408. https://doi.org/10.1006/meth.2001.1262.

Lopez-Delacalle, M., Silva, C.J., Mestre, T.C., Martinez, V., Blanco-Ulate, B., Rivero, R.M., 2021. Synchronization of proline, ascorbate and oxidative stress pathways under the combination of salinity and heat in tomato plants. Environ. Exp. Bot. 183, 104351 https://doi.org/10.1016/j.envexpbot.2020.104351.

Løvdal, T., Lillo, C., 2009. Reference gene selection for quantitative real-time PCR normalization in tomato subjected to nitrogen, cold, and light stress. Anal. Biochem. 387, 238–242. https://doi.org/10.1016/j.ab.2009.01.024.

Marín-Navarro, J., Moreno, J., 2003. Modification of the proteolytic fragmentation pattern upon oxidation of cysteines from Ribulose 1,5-bisphosphate carboxylase/oxygenase. Biochemistry 42, 14930–14938. https://doi.org/10.1021/bi035713j.

Mariz-Ponte, N., Mendes, R.J., Sario, S., Correia, C.V., Correia, C.M., Moutinho-Pereira, J., et al., 2021. Physiological, biochemical and molecular assessment of UV-A and UV-B supplementation in Solanum lycopersicum. Plants 10. https://doi.org/10.3390/plants10050918.

Mathur, S., Agrawal, D., Jajoo, A., 2014. Photosynthesis: response to high temperature stress. J. Photochem. Photobiol. B Biol. 137, 116–126. https://doi.org/10.1016/j.jphotobiol.2014.01.010.

Maurya, V.K., Srinvasan, R., Ramesh, N., Anbalagan, M., Gothandam, K.M., 2015. Expression of carotenoid pathway genes in three *capsicum varieties* under salt stress. Asian J Crop Sci 7, 286–294. https://doi.org/10.3923/ajcs.2015.286.294.

Muller, P., Li, X.P., Niyogi, K.K., 2001. Non-photochemical quenching. A response to excess light energy. Plant Physiol. 125, 1558–1566. https://doi.org/10.1104/pp.125.4.1558.

Murashige, T., Skoog, F., 1962. A revised medium for rapid growth and bio assays with tobacco tissue cultures. Physiol. Plantarum 15, 473–497. https://doi.org/10.1111/j.1399-3054.1962.tb08052.x.

Olmo, M., Alburquerque, J.A., Barrón, V., del Campillo, M.C., Gallardo, A., Fuentes, M., et al., 2014. Wheat growth and yield responses to biochar addition under Mediterranean climate conditions. Biol. Fertil. Soils 50, 1177–1187. https://doi.org/10.1007/s00374-014-0959-y.

Parihar, P., Singh, S., Singh, R., Singh, V.P., Prasad, S.M., 2015. Effect of salinity stress on plants and its tolerance strategies: a review. Environ. Sci. Pollut. Res. 22, 4056–4075. https://doi.org/10.1007/s11356-014-3739-1.

Park, C.J., Seo, Y.S., 2015. Heat shock proteins: a review of the molecular chaperones for plant immunity. Plant Pathol. J. 31, 323–333. https://doi.org/10.5423/PPJ.RW.08.2015.0150.

Poorter, H., Garnier, E., 2007. Ecological significance of inherent variation in relative growth rate and its components. In: Funct. Plant Ecol., pp. 67–100. CRC press.

Pospíšil, P., Prasad, A., 2014. Formation of singlet oxygen and protection against its oxidative damage in Photosystem II under abiotic stress. J. Photochem. Photobiol. B Biol. 137, 39–48. https://doi.org/10.1016/j.jphotobiol.2014.04.025.

Raja, V., Qadir, S.U., Alyemeni, M.N., Ahmad, P., 2020. Impact of drought and heat stress individually and in combination on physio-biochemical parameters, antioxidant responses, and gene expression in *Solanum lycopersicum*. 3 Biotech 10, 208. https://doi.org/10.1007/s13205-020-02206-4.

Rao, S., Das, J.R., Mathur, S., 2021. Exploring the master regulator heat stress transcription factor HSFA1a-mediated transcriptional cascade of HSFs in the heat stress response of tomato. J. Plant Biochem. Biotechnol. 30, 878–888. https://doi.org/10.1007/s13562-021-00696-8.

Rivero, R.M., Mestre, T.C., Mittler, R., Rubio, F., Garcia-Sanchez, F., Martinez, V., 2014. The combined effect of salinity and heat reveals a specific physiological, biochemical

and molecular response in tomato plants. Plant Cell Environ. 37, 1059–1073. https://doi.org/10.1111/pce.12199.
Santos, C.V., 2004. Regulation of chlorophyll biosynthesis and degradation by salt stress in sunflower leaves. Sci. Hortic. (Amst.) 103, 93–99. https://doi.org/10.1016/j.scienta.2004.04.009.
Schindelin, J., Arganda-Carreras, I., Frise, E., Kaynig, V., Longair, M., Pietzsch, T., et al., 2012. Fiji: an open-source platform for biological-image analysis. Nat. Methods 9, 676–682. https://doi.org/10.1038/nmeth.2019.
Singh, J., Thakur, J.K., 2018. Photosynthesis and abiotic stress in plants. In: Vats, S. (Ed.), Biot. Abiotic Stress Toler. Springer Singapore, Plants, Singapore, pp. 27–46. https://doi.org/10.1007/978-981-10-9029-5_2.
Soares, C., Branco-Neves, S., de Sousa, A., Pereira, R., Fidalgo, F., 2016. Ecotoxicological relevance of nano-NiO and acetaminophen to *Hordeum vulgare* L.: combining standardized procedures and physiological endpoints. Chemosphere 165, 442–452. https://doi.org/10.1016/J.CHEMOSPHERE.2016.09.053.
Soares, C., Pereira, R., Martins, M., Tamagnini, P., Serôdio, J., Moutinho-Pereira, J., et al., 2020. Glyphosate-dependent effects on photosynthesis of *Solanum lycopersicum* L.—an ecophysiological, ultrastructural and molecular approach. J. Hazard Mater. 398, 122871 https://doi.org/10.1016/j.jhazmat.2020.122871.
Sousa, B., Rodrigues, F., Soares, C., Martins, M., Azenha, M., Lino-Neto, T., et al., 2022. Impact of combined heat and salt stresses on tomato plants—insights into nutrient uptake and redox homeostasis. Antioxidants 11. https://doi.org/10.3390/antiox11030478.
Spormann, S., Nadais, P., Sousa, F., Pinto, M., Martins, M., Sousa, B., et al., 2023. Accumulation of proline in plants under contaminated soils—are we on the same page? Antioxidants 12. https://doi.org/10.3390/antiox12030666.
Spreitzer, R.J., Salvucci, M.E., 2002. RUBISCO: structure, regulatory interactions, and possibilities for a better enzyme. Annu. Rev. Plant Biol. 53, 449–475. https://doi.org/10.1146/annurev.arplant.53.100301.135233.
Sun, Y.L., Li, F., Su, N., Sun, X.L., Zhao, S.J., Meng, Q.W., 2010. The increase in unsaturation of fatty acids of phosphatidylglycerol in thylakoid membrane enhanced salt tolerance in tomato. Photosynthetica 48, 400–408. https://doi.org/10.1007/s11099-010-0052-1.
Suzuki, N., Rivero, R.M., Shulaev, V., Blumwald, E., Mittler, R., 2014. Abiotic and biotic stress combinations. New Phytol. 203, 32–43. https://doi.org/10.1111/nph.12797.
von Caemmerer, S., Farquhar, G.D., 1981. Some relationships between the biochemistry of photosynthesis and the gas exchange of leaves. Planta 153, 376–387. https://doi.org/10.1007/BF00384257.
Wahid, A., Gelani, S., Ashraf, M., Foolad, M.R., 2007. Heat tolerance in plants: an overview. Environ. Exp. Bot. 61, 199–223. https://doi.org/10.1016/j.envexpbot.2007.05.011.
Yin, Z., Lu, J., Meng, S., Liu, Y., Mostafa, I., Qi, M., et al., 2019. Exogenous melatonin improves salt tolerance in tomato by regulating photosynthetic electron flux and the ascorbate–glutathione cycle. J. Plant Interact. 14, 453–463. https://doi.org/10.1080/17429145.2019.1645895.
Yoshioka, M., Yamamoto, Y., 2011. Quality control of Photosystem II: Where and how does the degradation of the D1 protein by FtsH proteases start under light stress? – Facts and hypotheses. J. Photochem. Photobiol. B Biol. 104, 229–235. https://doi.org/10.1016/j.jphotobiol.2011.01.016.
Yu, W., Wang, L., Zhao, R., Sheng, J., Zhang, S., Li, R., et al., 2019. Knockout of *SlMAPK3* enhances tolerance to heat stress involving ROS homeostasis in tomato plants. BMC Plant Biol. 19, 354. https://doi.org/10.1186/s12870-019-1939-z.
Zahra, N., Al Hinai, M.S., Hafeez, M.B., Rehman, A., Wahid, A., Siddique, K.H.M., et al., 2022. Regulation of photosynthesis under salt stress and associated tolerance mechanisms. Plant Physiol. Biochem. 178, 55–69. https://doi.org/10.1016/j.plaphy.2022.03.003.
Zahra, N., Hafeez, M.B., Ghaffar, A., Kausar, A., Zeidi, M Al, Siddique, K.H.M., et al., 2023. Plant photosynthesis under heat stress: effects and management. Environ. Exp. Bot. 206, 105178 https://doi.org/10.1016/j.envexpbot.2022.105178.
Zhang, Q.Y., Wang, L.Y., Kong, F.Y., Deng, Y.S., Li, B., Meng, Q.W., 2012. Constitutive accumulation of zeaxanthin in tomato alleviates salt stress-induced photoinhibition and photooxidation. Physiol. Plantarum 146, 363–373. https://doi.org/10.1111/j.1399-3054.2012.01645.x.
Zhang, H., Zhu, J., Gong, Z., Zhu, J.K., 2021. Abiotic stress responses in plants. Nat. Rev. Genet. https://doi.org/10.1038/s41576-021-00413-0.
Zhou, X., Zhao, H., Cao, K., Hu, L., Du, T., Baluška, F., et al., 2016. Beneficial roles of melatonin on redox regulation of photosynthetic electron transport and synthesis of D1 protein in tomato seedlings under salt stress. Front. Plant Sci. 7 https://doi.org/10.3389/fpls.2016.01823.
Zribi, L., Fatma, G., Fatma, R., Salwa, R., Hassan, N., Néjib, R.M., 2009. Application of chlorophyll fluorescence for the diagnosis of salt stress in tomato "Solanum lycopersicum (variety Rio Grande).". Sci. Hortic. (Amst.) 120, 367–372. https://doi.org/10.1016/j.scienta.2008.11.025.